# Peptide and Peptide Mimetic Inhibitors of Antigen Presentation by HLA-DR Class II MHC Molecules. Design, Structure−Activity Relationships, and X-ray Crystal Structures

David R. Bolin, Amy L. Swain,*,§ Ramakanth Sarabu, Steven J. Berthel, Paul Gillespie, Nicholas J. S. Huby, Raymond Makofske, Lucja Orzechowski, Agostino Perrotta, Katherine Toth, Joel P. Cooper, Nan Jiang, Fiorenza Falcioni, Robert Campbell, Donald Cox, Diana Gaizband, Charles J. Belunis, Damir Vidovic, Kouichi Ito, Robert Crowther, Ursula Kammlott, Xiaolei Zhang, Robert Palermo, David Weber, Jeanmarie Guenot, Zoltan Nagy, and Gary L. Olson*,†

*Roche Research Center, Hoffmann-La Roche Inc., 340 Kingsland Street, Nutley, New Jersey 07110*

*Received January 26, 2000*

Molecular features of ligand binding to MHC class II HLA-DR molecules have been elucidated through a combination of peptide structure−activity studies and structure-based drug design, resulting in analogues with nanomolar affinity in binding assays. Stabilization of lead compounds against cathepsin B cleavage by *N*-methylation of noncritical backbone NH groups or by dipeptide mimetic substitutions has generated analogues that compete effectively against protein antigens in cellular assays, resulting in inhibition of T-cell proliferation. Crystal structures of four ternary complexes of different peptide mimetics with the rheumatoid arthritis-linked MHC DRB1*0401 and the bacterial superantigen SEB have been obtained. Peptide−sugar hybrids have also been identified using a structure-based design approach in which the sugar residue replaces a dipeptide. These studies illustrate the complementary roles played by phage display library methods, peptide analogue SAR, peptide mimetics substitutions, and structure-based drug design in the discovery of inhibitors of antigen presentation by MHC class II HLA-DR molecules.

## Introduction

MHC class II molecules are specialized peptide receptors that bind fragments of extracellular proteins and present them on the surface of antigen-presenting cells for recognition by T-cell receptors. Recognition of a foreign peptide antigen triggers T-cell proliferation, cytokine release, and antibody production and is critical for normal immune responses. However, in autoimmune disorders such as rheumatoid arthritis (RA), multiple sclerosis, and diabetes mellitus, peptide fragments of normal cellular proteins in complex with an MHC class II molecule are mistakenly recognized as foreign, leading to the destruction of normal tissues and chronic autoimmune disease.[1] Genetic susceptibility in autoimmune diseases is linked to specific alleles of the MHC complex.[2] For example, in RA, >90% of patients carry genes for MHC class II DRB1*0101 (DR1), DRB1*0401 (DR4), DRB1*0404, and DRB1*0405, whereas multiple sclerosis is associated with DRB1*1501, and diabetes with DQ alleles. The hypotheses of autoantigen presentation and genetic linkage in autoimmune disease have led to the concept[3] of selectively inhibiting antigen presentation by competitive blockade of the peptide binding site of a disease-associated MHC molecule using a nonantigenic ligand. Inhibition of antigen binding to HLA-DR molecules, for example, could be a viable approach to the treatment of rheumatoid arthritis and other DR-associated autoimmune diseases.

At the molecular level, the crystal structures of several MHC class II molecules with bound peptides have been determined and the general features of the molecular recognition between antigenic peptide and the binding site on the class II molecule have been described.[4] MHC:T-cell receptor complex structures have also been determined, demonstrating the points of interaction and nature of T-cell receptor binding.[5] The peptide binding motifs for heptapeptides binding to DR alleles have also been elucidated through phage display libraries and synthetic peptides.[6] These data have been employed to assemble peptide sequences that exhibit nanomolar affinity for binding to isolated MHC class II DR molecules (e.g., Ac-YRAMATL-$NH_2$). However, the simple peptides based on this motif, or longer, partially stabilized sequences, e.g., a(Cha)AAAKTAAAAa-$NH_2$,[7] are not able to inhibit T-cell responses to protein antigens in vitro and have not shown in vivo inhibition in animal models due to problems inherent in peptide structures.[8]

The failure of these peptide inhibitors appears to result from the inability of simple peptide competitors to survive in the environment of antigen-presenting cells (APCs) (see Figure 1). In antigen processing, an exogenous protein is endocytosed by APCs and cleaved within acidic endosomal compartments into 9−30 residue fragments by proteases of the cathepsin family. MHC class II molecules, preassociated with another protein, the "invariant chain" (Ii), enter the endosomal compartment for enzymatic processing. Here the invari-

* Corresponding authors. E-mail: golson@provid-ppi.com and swaina@ncrr.nih.gov.
† Present address: Provid Research, 10 Knightsbridge Rd, Piscataway, NJ 08854. Tel: (732) 457-0100. Fax: (732) 457-0454.
§ Present address: National Center for Research Resources, National Institutes of Health, 6705 Rockledge Dr, Bethesda, MD 20892. Tel: (301) 435-0752.

10.1021/jm000034h CCC: $19.00 
Published on Web 05/12/2000

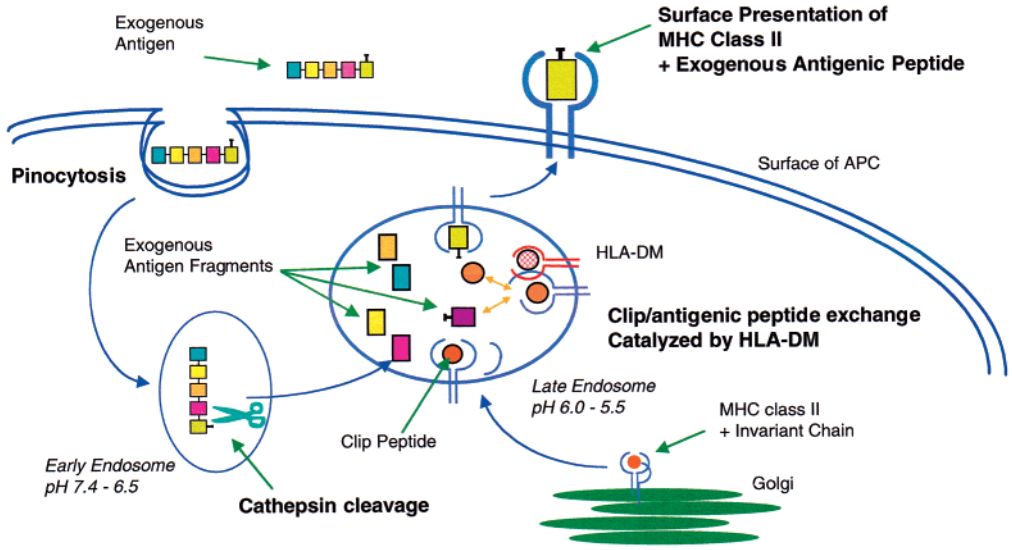


**Figure 1.** Antigen processing and loading of MHC class II.

ant chain is cleaved, leaving a residual 24-mer peptide ("CLIP") bound in the MHC binding site. The CLIP peptide and antigenic fragments are exchanged under the catalysis of another MHC molecule, HLA-DM, resulting in the loading of the MHC with the highest affinity binding peptides.[9] Once loaded, the MHC−peptide complex translocates to the cell surface, where it is presented for recognition by the T-cell receptor. Cell surface exchange of peptide ligands bound to MHC is thought to be very slow, making it unlikely for competitive binding with a high-affinity ligand to occur on the cell surface. Thus any potential competitor peptide ligands designed to block antigen presentation must be able to (a) enter the APC, (b) survive processing enzymes, and (c) compete for binding with CLIP in order to express their activity as competitor ligands. This extensive processing and loading pathway demands that competitor peptides be selected not only on the basis of their affinity for an isolated, "empty", MHC molecule in a binding assay but also for their requisite stability and physicochemical properties if they are to compete for binding within the cellular loading environment. The efficient endocytotic process of antigen-presenting cells obviates the need for competitor ligands to be transported across cell membranes, but they still must have suitable bioavailability, stability, and pharmacokinetics to become useful drugs. These criteria present challenges for peptide-like molecules. One approach via fully unnatural ligands binding to MHC class II has been presented, but the compounds did not show activity in cellular models.[10]

In this report, we describe the design of peptidomimetic ligands that exhibit high-affinity binding to HLA-DR molecules. These inhibitors have been designed on the basis of the peptide binding motifs for several DR allotypes identified by phage display library studies and via peptide SAR analysis. The published X-ray crystal structure of the DRB1*0101 allotype with viral peptide antigen HA (306−318) (PKYVKQNTLKLAT) in the binding site was used as an initial step in structure-based drug design. Using SAR and properties of the consensus heptapeptide (Ac-YRAMATL-$NH_2$) derived from phage sequence data, analogues have been optimized for competition for peptide antigen binding within compartments of antigen-presenting cells. In addition to seeking ligands with high affinity for RA-linked DR allotypes, we optimized compounds for stability against cathepsin cleavage, small molecular size, and minimization of peptide-like features. We also present X-ray crystal structures of complexes of four of our novel ligands with HLA-DR4 (DRB1*0401), confirming structure-based design hypotheses and suggesting further refinements. The compounds we discuss have demonstrated inhibition of T-cell proliferation in response to protein antigens, indicating their ability to be taken up by APCs and to be loaded onto MHC class II molecules in competition with antigenic peptide[11] fragments of ovalbumin and hen egg white lysozyme. The design process, structure−activity relationships, and structural information obtained may be useful in optimization of mimetics for in vivo activity or in extension of the approach to other targets.

## X-ray Crystallography

To complement the design process, the crystal structures of one peptide and three peptidomimetics bound to DR4, in complex with streptococcal enterotoxin B superantigen (SEB), were determined at 2.0 or 2.45 Å resolution (Figure 2a). The electron density for DR4 was clearly interpretable and continuous with the exception of a loop of residues 105−112 at the distal end of the beta subunit. This disorder is likely due to motion of the loop in the crystal. The electron density for SEB was quite clear except for one loop from residue 99 to 108, which is disordered. In all of the structures, the SEB does not appear to interfere with the DR4 antigen binding site and was included in the complexes as a vehicle to form crystals of DR4 with novel compounds that diffract well. The compounds are observed in an extended conformation in the binding cleft of DR4 as expected and as observed by other investigators.[4] Specific interactions between DR4 and the inhibitors correlate with the observed inhibitory activities and support the structure-based design methodology. Details of interactions at each binding subsite will be discussed further below.

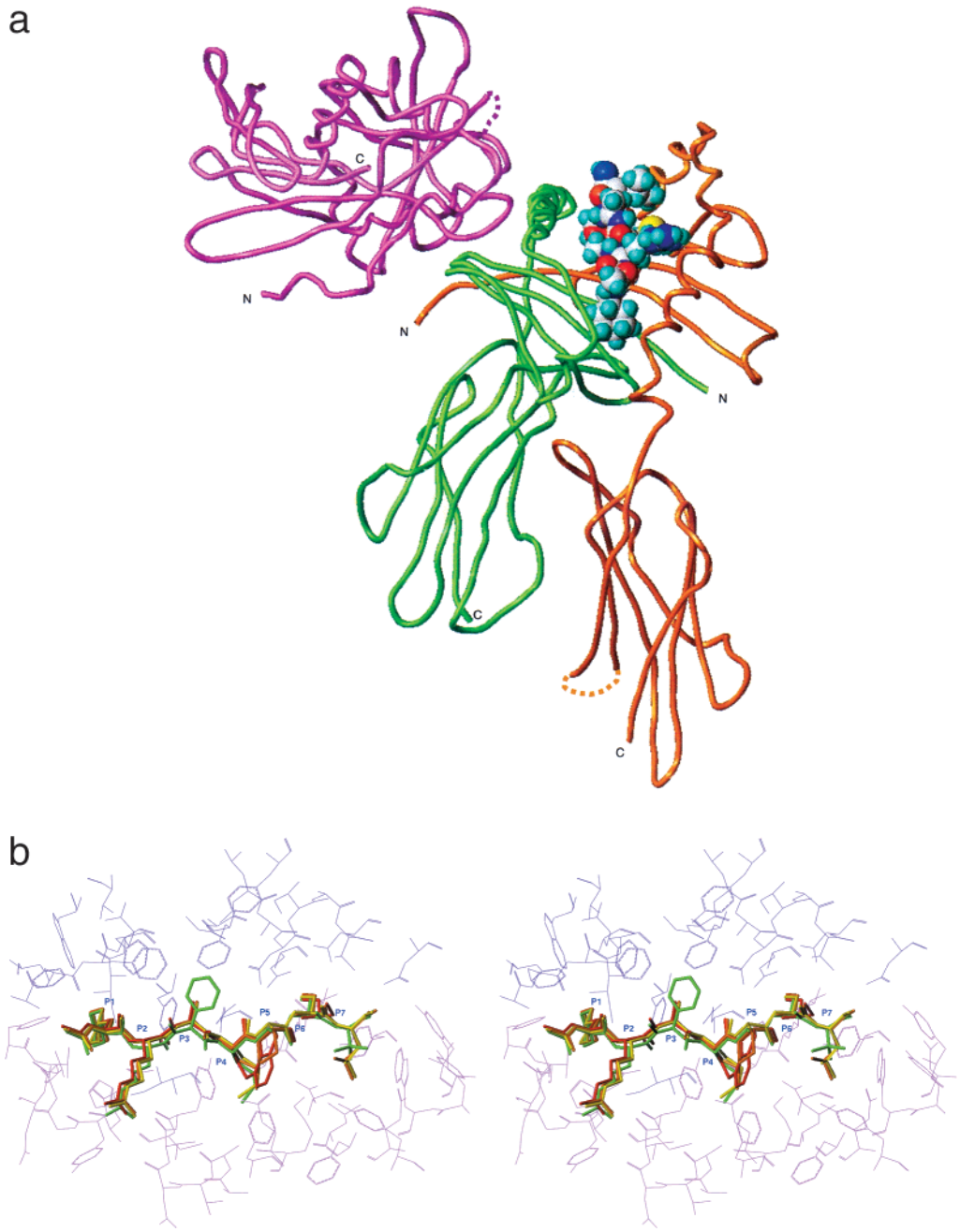


**Figure 2.** (a) $C_\alpha$ trace of DR4 in complex with SEB (magenta). The α chain of DR4 is shown in green and the $\beta$ chain in orange. SEB does not appear to distort the binding groove. The peptide, **28**, is shown in space-filling atoms with the p1 (Cha) residue in front. (b) Stereoview of the DR4 peptide binding site. Orientation is top down on the binding groove and ca. 90° rotated from that in part a. Residues within a 7 Å radius of the bound peptide are shown in fine lines, with the α chain in purple (residues α3−81) and the $\beta$ chain in magenta (residues $\beta$ 5−85). Compounds **28** (yellow), **72** (orange), **73** (red), and **60** (green) are overlaid by superimposing the DR4 atoms that compose the binding groove shown. The binding subsites for p1−p7 are labeled.

## Design and SAR of Peptide Analogues

We initiated design efforts with peptide and peptidomimetic ligands to obtain quantitative binding data and to establish the SAR for the key binding sites. We set out to identify compounds that have the backbone recognition and side chain anchor features common to all RA-associated DR alleles. The binding motif information generated previously by panning M13 phage expressed random peptide libraries[12] is listed in Table 1. These data show the importance of residues at p1, p2, p4, p6, and p7 on binding. This information, in combination with the crystal structure of the DRB1*0101:HA complex, which indicated the presence of the same side chain recognition sites, led to the selection of Ac-YRAMASL-$NH_2$ as an initial consensus peptide. This compound exhibited 41 nM ($IC_{50}$) binding affinity to DRB1*0401 and 218 nM ($IC_{50}$) affinity for DRB1*0101.[13] The crystal structure of the DRB1*0101:HA(306−318) complex[4a] revealed, in addition to specific interactions with peptide ligand side chains, a network of backbone recognition hydrogen bonds that are important for binding. The role of this H-bond network in molecular recognition could not have been elucidated by phage display technology (in which all phages vary only in side chains). In particular, the peptide backbone at p2 and p4 is making hydrogen-bond contacts with side chain

**Table 1.** Sequence Motifs of Peptides Binding to MHC Class II DR Molecules Elucidated by M13 Phage Libraries and Synthetic Peptide Libraries (Hammer et al.[11])

| | residue at peptide position | | | | | | | | |
|---|---|---|---|---|---|---|---|---|---|
| DRB1 | 1 | 2 | 3 | 4 | 5 | 6 | 7 | 8 | 9 |
| *0101 | Y<br>F<br>W | R | − | M<br>L | − | A<br>G<br>S | L<br>I<br>V | − | L<br>M<br>A |
| *0401 | W<br>Y<br>F | R | − | M<br>A<br>V<br>L | − | T<br>S<br>N | L<br>Q<br>M<br>N<br>I<br>V | − | − |
| *0404 | I<br>L<br>M<br>F<br>V | R | − | M<br>I<br>L<br>F | − | T<br>N<br>S<br>V | M<br>N<br>L<br>I | − | − |
| *0405 | Y<br>F<br>W | R | − | M<br>F | − | N<br>S<br>T | F<br>Y<br>N<br>L | − | E<br>D |

residues in the binding pocket (Gln82, Asn62 + Gln9, respectively). These contacts (see Figure 3) include amide NHs that are shielded from solvent; we provide evidence that they should be maintained in analogues.

**p1.** The phage-derived peptides and HA (306−318) revealed a number of side chain recognition sites, or "anchors." At position 1, a deep hydrophobic pocket is observed in the binding site, where Tyr, Phe, and Trp are observed to be preferred in DRB1*0101 and -*0401. Due to a Gly to Val residue change at $\beta$-86 in the bottom of the p1 pocket in DRB1*0404 (RA linked) and -*0402 (not RA linked), the larger Tyr and Trp side chains are not able to bind to these alleles. This information led to our selection of cyclohexylalanine (Cha) as a consensus position 1 anchor for peptide SAR studies. The Ac-(Cha)-RAMASL-$NH_2$ peptide (**1**) exhibited 23−80 nM affinity for DRB1*0101, -*0401, -*0404, -*0405, and -*0402 alleles. Examination of a model of **1** docked into either the DRB1*0101 or DRB1*0401 sites indicated that there might be additional space in the pocket to accommodate groups larger than Cha. With this compound as a reference point, we began a detailed exploration of the p1 group to exploit this deep pocket for additional binding affinity; p1 analogues were prepared and compared with the reference Ac-(Cha)RAMASL-$NH_2$ peptide [DRB1*0401 $IC_{50} = 0.039 \pm 0.003$ $\mu$M ($n = 55$); DRB1*0101 $IC_{50} = 0.068 \pm 0.006$ $\mu$M ($n = 55$)]. In the tables, relative potencies for p1 and other analogues are given to account for interassay variability. Among the p1 analogues synthesized, higher binding affinity to DRB1*0401 was observed (Table 2) for homocyclohexylalanine (**3**), 4-methylcyclohexylalanine (cis and trans) (**4**, **5**), norbornyl- (**2**) and cyclooctylalanine, 3,4-methylenedioxyphenylalanine (**8**), and 3-iodo- (**9**) and 3-fluorophenylalanine (**11**). Only the cycloaliphatic analogues bound with high affinity to DRB1*0101, due to its shallower pocket. Nevertheless, the additional binding affinity gained by these more complex structural types relative to Cha was not more than 1.7-fold, so we continued to use cyclohexylalanine as a position 1 replacement for structure−activity studies, with the option to exchange it for one of the other cycloaliphatic derivatives at a later stage. In the compounds bound to DRB1*0401 in our crystal structures, all have Cha at p1 (see Figure 2b) and the cyclohexyl rings are observed in an orientation approximately perpendicular to the plane of the tyrosine ring at p1 of HA in DRB1*0101. This rotation may help explain the increased affinity of compound **2**, which has norbornylalanine at p1; such an orientation would allow sufficient space to accommodate the bicyclic ring system of this residue. The N-terminal acetyl group is observed to be in the same orientation for all four crystal structures. As seen in the HA peptide for the backbone NH of the p0 residue (Lys), the Cha amide nitrogen forms a hydrogen bond with the carbonyl oxygen of Ser53 on the alpha chain, and the carbonyl oxygen of the acetyl group forms a hydrogen bond with N$\epsilon$2 of His81 on the beta chain. These interactions contribute to binding affinity as noted by the decreased affinity of desamino analogues (data not shown).

**p2.** At p2, the phage library indicates a preference for Arg, whereas Val is located in this position in the HA peptide, where there is a nearby positive charge located at p0 (Lys). In the context of Ac-(Cha)-containing heptapeptides, Arg or other charged amino acids [Orn (**13**), Lys (**15**), $Orn(Me)_2$ (**14**), $Lys(Me)_2$ (**16**)] at p2 were effective binders to DRB1*0401 and DRB1*0101, but groups other than Arg showed lower potency toward DRB1*0101 (Table 3). In our four crystal structures, Arg2 is present in each ligand, and the Arg side chain extends out of the binding groove, making van der Waals contacts with protein atoms of the beta chain as well as an interesting $\pi$-stacking interaction between the guanidinium group and the imidazole ring of His81 of the beta chain of DR4. We conclude that it is likely that the hydrophobic interactions along the arginine side chain and interactions with His 81 may be the essential pharmacophore elements of this side chain. Branched amino acids, chosen to incorporate the $\beta$-alkyl group corresponding to the Val2 residue of the HA peptide (as in **12** and **17**), were also acceptable, particularly when there was a further modification at p3 (i.e., *N*-methyl-Phg). Large hydrophobic, small nonpolar, or negatively charged side chain residues at p2 tended to decrease affinity significantly. The allo-Ile group in **17** incorporates both the beta branch and the hydrocarbon portion of Arg. It also was a high affinity replacement when an aminoalkyl chain corresponding to the HA peptide position 0 lysine was substituted for the terminal acetyl group, i.e., in $H_2N(CH_2)_4CO$-(Cha)-(aIle)AMASL-$NH_2$ (**18**). The unnatural part of this ligand mimics the KYV sequence in the HA peptide (P**KYV**KQNTLKLAT), and the modified heptapeptide **18** is more potent in binding than the 13-mer HA peptide (7.25- and 2.24-fold vs DRB1*0401 and DRB1*0101, respectively). Another such approach to mimic the HA peptide has recently been reported using dipyrrolinones as a replacement for the VKQN sequence (p2−p4) of the HA peptide.[14,15]

**p3.** Initial studies of the position 3 site in the phage display studies did not reveal any strong preferences, although in synthetic peptide analogues Pro was preferred over Ala, consistent with the twisted helical structure seen in the DR1:HA peptide crystal structure.[4] However, we felt that a hydrophobic patch formed by a cluster of aromatic residues near p3 as observed in the DR1:HA crystal structure could represent a novel site

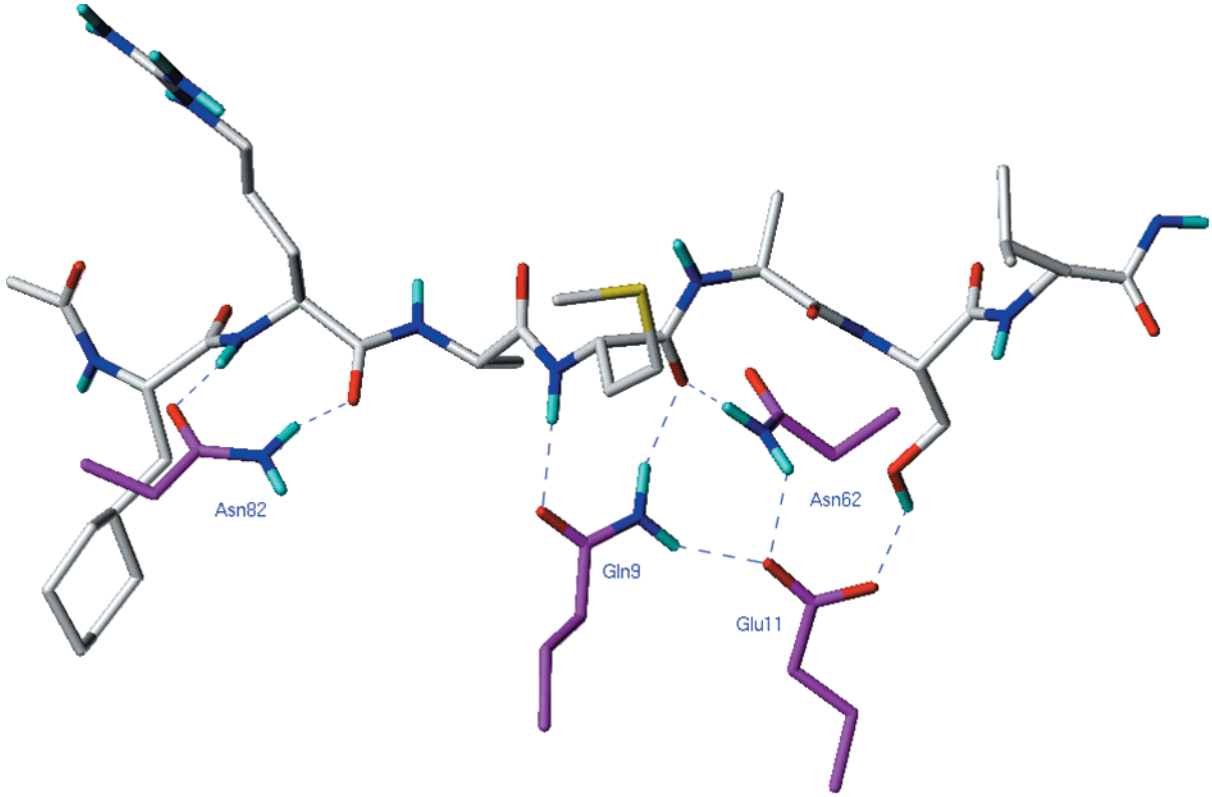


**Figure 3.** Hydrogen-bond contacts in the structure of **28** bound to DR4 showing interactions with Asn82 and the p2 Arg backbone NH and CO as well as the p4 Met backbone interacting with the network of Gln-9, Asn-62, and Glu-11. The backbone NHs and COs of p3, p5, p6, and p7 are not making H-bonds with DR4. The data are consistent with that of the HA peptide in DR1 (Stern and Wiley[4]).

**Table 2.** P1 Analogues Having Higher Affinity in DRB1*0401 Binding Assay Than **1**

| | | mean relative potency[a] | |
|---|---|---|---|
| no. | structure | DRB1-*0401 | DRB1-*0101 |
| **2** | Ac-(L-Nba)RAMASL-$NH_2$ | 1.71 | 0.52 |
| **3** | Ac-(L-hCha)RAMASL-$NH_2$ | 1.19 | 1.25 |
| **4** | Ac-(p$CH_3$-Cha)RAMASL-$NH_2$[b] | 0.93 | 1.17 |
| **5** | Ac-(p$CH_3$-Cha)RAMASL-$NH_2$[b] | 1.71 | 1.37 |
| **6** | Ac-(2-(S)-*exo*-L-Nba)RAMASL-$NH_2$ | 0.92 | 0.96 |
| **7** | Ac-(2-(R)-*exo*-L-Nba)RAMASL-$NH_2$ | 1.53 | 1.31 |
| **8** | Ac-(Mdp)RAMASL-$NH_2$ | 1.65 | 1.31 |
| **9** | Ac-(L-m-I-Phe)RAMASL-$NH_2$ | 1.56 | 0.61 |
| **10** | Ac-(2-(S)-Bcoa)RAMASL-$NH_2$ | 1.22 | 0.68 |
| **11** | Ac-(L-m-F-Phe)RAMASL-$NH_2$ | 1.19 | 0.17 |

[a] Ratio of $IC_{50}$ values for Ac-(Cha)RAMASL-$NH_2$ and listed sequence. Values greater than 1 are more potent. [b] Separated cis and trans isomers.

for interaction with appropriate *unnatural* side chain hydrophobic groups. Consequently, we explored analogues of phenylglycine [Phg (**20**), *N*-methylPhg (**21**), and derivatives] and several conformationally restricted aromatic compounds [Tic (**23**), Disc (**22**)]. These, along with a series of blocked Cys compounds [Cys(Acm) (**24**)], a series of S-alkylated Cys derivatives, and corresponding Met homologues all yielded compounds with enhanced binding affinity (up to ca. 3-fold relative to the Ala peptide). Our crystal structure with compound **60** has MePhg at position 3. The phenyl group is enveloped by an aromatic cluster (Figure 4) making close contacts with Phe22 and Phe54 and Gly58 of the α chain. As a result, the backbone of this compound is shifted slightly compared to the others that have Ala at that position (Figure 5).

**Table 3.** Series of Single Substitution Analogues of the Heptapeptide **1**

| | | mean relative potency[a] | |
|---|---|---|---|
| no. | structure | DRB1 *0401 | DRB1 *0101 |
| **12** | Ac-(Cha)VAMASL-$NH_2$ | 0.91 | 0.46 |
| **13** | Ac-(Cha)OAMASL-$NH_2$ | 0.67 | 0.09 |
| **14** | Ac-(Cha)O$(Me)_2$AMASL-$NH_2$ | 0.38 | 0.29 |
| **15** | Ac-(Cha)KAMASL-$NH_2$ | 0.45 | 0.12 |
| **16** | Ac-(Cha)K$(Me)_2$AMASL-$NH_2$ | 0.62 | 0.14 |
| **17** | Ac-(Cha)(aIle)AMASL-$NH_2$ | 1.27 | 0.41 |
| **18** | $NH_2(CH_2)_4$CO-(Cha)(aIle)AMASL-$NH_2$ | 1.16 | 1.36 |
| **19** | Ac-(Cha)RPMASL-$NH_2$ | 1.85 | 0.56 |
| **20** | Ac-(Cha)R(Phg)MASL-$NH_2$ | 1.10 | 1.34 |
| **21** | Ac-(Cha)R(MePhg)MASL-$NH_2$ | 2.32 | 0.29 |
| **22** | Ac-(Cha)R(Disc)MASL-$NH_2$ | 0.50 | 0.31 |
| **23** | Ac-(Cha)R(Tic)MASL-$NH_2$ | 0.20 | 0.43 |
| **24** | Ac-(Cha)R(CAcm)MASL-$NH_2$ | 1.36 | 1.18 |
| **25** | Ac-(Cha)RA(Nle)ASL-$NH_2$ | 0.40 | 0.77 |
| **26** | Ac-(Cha)RAIASL-$NH_2$ | 1.01 | 0.36 |
| **27** | Ac-(Cha)RALASL-$NH_2$ | 0.54 | 0.55 |
| **28** | Ac-(Cha)RAM(CAcm)SL-$NH_2$ | 1.73 | 1.45 |
| **29** | Ac-(Cha)RAMPSL-$NH_2$ | 0.70 | 1.37 |
| **30** | Ac-(Cha)RAM(Pip)SL-$NH_2$ | 1.08 | 0.55 |
| **31** | Ac-(Cha)RAM(β-PhPro)SL-$NH_2$ | 1.04 | 0.92 |
| **32** | Ac-(Cha)RAMAS(MeL)-$NH_2$ | 0.77 | 0.85 |
| **33** | Ac-(Cha)RAMAS(tLeu)-$NH_2$ | 1.46 | 1.64 |
| **34** | Ac-(Cha)RAMASL-N$(CH_3)_2$ | 1.60 | 1.40 |

[a] Ratio of $IC_{50}$ values for Ac-(Cha)RAMASL-$NH_2$ (**1**) and listed sequence. Values greater than 1 are more potent.

**p4.** Position 4 is a site where changes in charge may discriminate among RA-linked and unlinked alleles. This site in the MHC beta chain contains a positive charge at position 71 in DR alleles linked to RA [i.e., Lys (DRB1*0401) or Arg (DRB1*0101)], whereas it is a negatively charged Glu in DRB1*0402 (not linked to RA). From the phage library (see Table 1), position 4 of

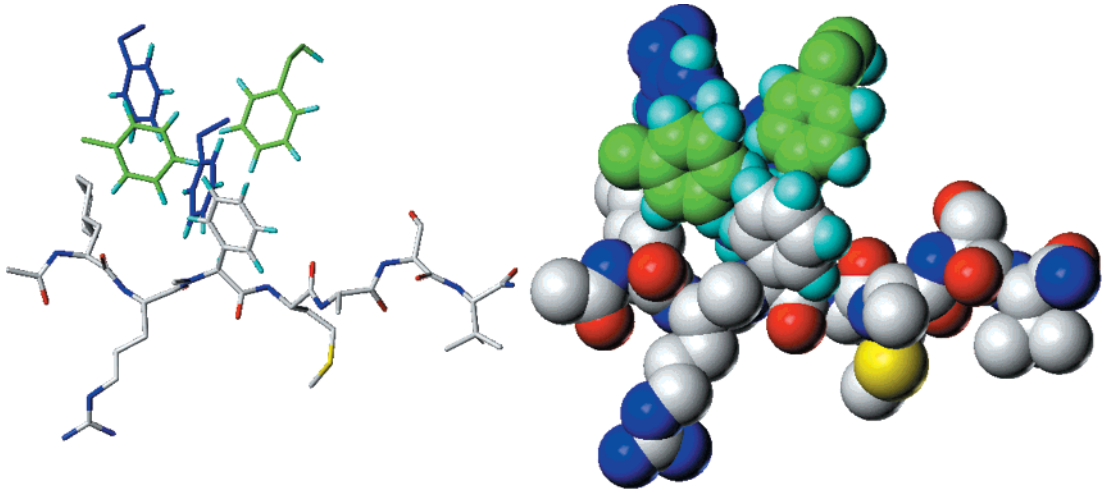

**Figure 4.** Figure of MePhg-containing analogue **60** in position 3. The aromatic ring of MePhg is shown to be in contact (within a 7 Å radius) with a cluster of aromatic residues (green, blue) and partially overlaps two of the aromatic rings (see space-filling model). Hydrogen positions are calculated.

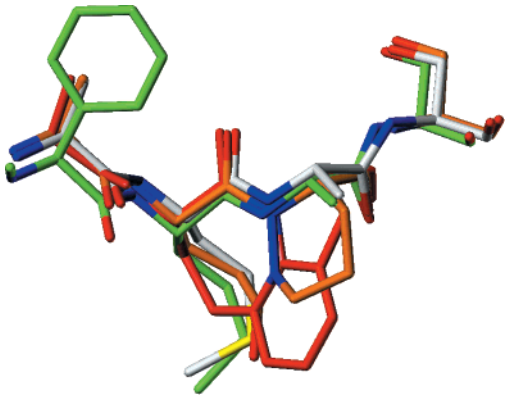

**Figure 5.** Overlay of positions 3−6 of **28** (carbons white), **72** (orange), **73** (red), and **60** (green). The compounds were overlaid by superposing the DR4 atoms that compose the binding groove. The side chain atoms of the Cys(Acm) group of **28** were omitted from the figure for clarity.

DRB1*0401 prefers neutral hydrophobic residues, e.g., Met, Ala, Val, Leu, whereas Gln is observed in this position in the HA peptide bound to DR1. In agreement with the Searle group,[13] including a negative charge at p4 of the ligand decreased binding to non-RA-linked alleles bearing negatively charged p71 residues. Extending this reasoning, we postulated that a productive $\pi$-cation interaction could be achieved between aromatic p4 groups and positively charged p71 side chains of RA-linked alleles (vide infra).

Position 4 was very sensitive to changes, with Met, Nle (**25**), Ile (**26**), and Leu (**27**) being the most potent individual amino acids at this site. Our crystal structures with compounds **28** and **60** both have Met at position 4, which is a fairly hydrophobic pocket. The Met side chain has van der Waals interactions with His13, Asp28, Lys71, Ala74, and Tyr78 of the beta chain. The p4 residue backbone is also involved in a critical hydrogen-bond network that restricts the NH and CO groups of the residue in a defined orientation in the site. These observations suggested that dipeptide mimetics intended to span positions 4 and 5, including those with aromatic groups (vide infra), would have to be carefully selected to meet the stringent requirements imposed on both the backbone and side chain interactions. Another successful solution has recently been reported using dipyrrolinones as a replacement for the VKQN sequence (p2−p4) of the HA peptide.[15]

**p5.** Analogues at position 5 tended to have binding affinity similar to, or somewhat reduced in potency relative to, the parent compound **1**. In the case of Acm-protected Cys residues and cyclic imino acids [Pro (**29**), Pip (**30**), $\beta$-Phe-Pro (**31**)], significant binding affinity was retained. The constrained amino acids presumably help orient the peptide backbone in the site, contributing to the overall free energy of binding. The Acm-protected Cys compound was found to stimulate T-cell proliferation, acting as an antigen rather than as an inhibitor (data not shown). This finding is consistent with the observation made from our crystal structure of **28** that the Cys(Acm) side chain projects out of the binding site, where it is exposed and available to the T-cell receptor. Because the C$\beta$ vector of p5 is directed toward the outside of the binding groove, one might expect a large side chain in this position to decrease binding capacity due to exposure of more atoms of the ligand to solvent. Indeed, 2-fold disorder is observed for the Cys(Acm) side chain, with each orientation making contacts with the protein. Nevertheless, the Cys(Acm) moiety has an enhanced effect on binding.

**p6.** At p6, DRB1*0101 prefers small, polar, neutral residues Ala, Ser, or Gly, whereas DRB1*0401 can accommodate Thr, Asn, and Ser. For p6, Ser appears to represent a compromise for both allotypes. In the crystal structure of DRB1*0101, the p6 Ser hydroxyl group is interacting with a hydrophilic patch that we considered could be important to complement our mimetics designs and led to our peptide sugar hybrids (vide infra). In our crystal structures with compounds **28**, **72**, and **60**, the p6 Ser OH is oriented in the same direction, making polar contacts with Glu11 and Asn62 of the $\alpha$ chain. Since studies revealed that truncation to a pentapeptide or tetrapeptide produced a decrease in binding (vide infra), a p6 hydroxyalkyl group was retained as a design feature in mimetic analogues. In the crystal structure with compound **73**, a hexapeptide mimetic, the C-terminal residue is serinol. Its bifunctional arm appendage is observed to be 2-fold disordered in the crystal structure.

**Table 4.** Series of C-Terminal Truncation Analogues

| | | mean relative potency[a] | | |
|---|---|---|---|---|
| no. | structure | DRB1-*0401 | DRB1-*0101 | DRB1-*0404 |
| **1** | Ac-(Cha)RAMASL-$NH_2$ | 1.00 | 1.00 | 1.00 |
| **35** | Ac-(Cha)RAMAS-$NH_2$ | 1.14 | 0.34 | 0.32 |
| **36** | Ac-(Cha)RAMA-$NH_2$ | 0.07 | 0.25 | 0.03 |
| **37** | Ac-(Cha)RAM-$NH_2$ | 0.01 | 0.05 | 0.005 |
| **38** | Ac-(Cha)RA-$NH_2$ | 0.000 | 0.000 | 0.000 |
| **39** | Ac-(Cha)RMM-$NH_2$ | 0.10 | 0.24 | 0.01 |

[a] Ratio of $IC_{50}$ values for Ac-(Cha)RAMASL-$NH_2$ and listed sequence. Values greater than 1 are more potent.

**p7.** The position 7 hydrophobic group (Leu in the lead peptide **1**) enhanced binding to multiple RA associated alleles but could be substituted by variants that are likely to be more resistant to carboxypeptidases, such as t-Leu (**33**), MeL (**32**), *N*,*N*-dialkyl amides (**34**), and descarboxy derivatives. We observe from the crystal structures of **28**, **72**, and **60** that the position 7 side chain is not buried, nor is it fully exposed to solvent. In compounds **28** and **72**, the residue is a leucine, whereas in compound **60** this residue is a *tert*-butyl glycine. The side chain projects off to the side of the axis of the peptide and, in the case where it is a leucine, makes van der Waals contacts with side chains Tyr47 and Leu67 of the beta subunit of DR4. The C-terminal amide group of these three compounds forms a hydrogen bond with the amide functionality of Asn69 on the alpha chain.

**Truncation Series.** Recent reports[15−18] have cited evidence that the heptapeptide length requirement for binding to two of the RA-linked alleles is not absolute. We have observed that the position 7 residue could be removed with a modest effect on binding activity, but (vide infra) the activity in cellular assays did not always follow this trend. To determine the number of residues at the C-terminus that could be eliminated and still retain binding, several truncated derivatives were synthesized with consecutive single amino acid deletions from the C-terminus. The relative binding affinities are illustrated in Table 4.

Elimination of a single residue, as for **35**, at position 7 of the binding motif, results in a two-thirds reduction in binding to *0101 and *0404, while not affecting *0401 binding. Further, removal of the position 6 residue as in **36**, previously shown to be important for *0401 binding, decreases binding to both *0401 and *0404, while not further affecting *0101 significantly. However, elimination of the next residue, yielding a tetrapeptide **37**, reduces binding for all three alleles to fractional activity. The tripeptide was inactive; however, substitution of p3 with Met in a tetrapeptide, **39**, gave a compound with moderate affinity for both *0401 and *0101 alleles.

## Biased Library Elaboration of Tetrapeptides Yields Peptide−Sugar Hybrids

To exploit the truncation results, we reasoned that the tetrapeptide Ac-(Cha)RMM-$NH_2$ (**39**) might be extended by non-amino-acid residues to reach the interesting interaction sites for the Ser hydroxyl group and the hydrophobic site where the Leu binds at position 7. For this purpose, a three-dimensional substructure search of commercially available non-peptide amino compounds was conducted using SYBYL Unity with the criteria that the compound must have a hydrogen-bond donor OH group and a hydrophobic atom (mimicking a part of the Leu7 chain) at distances consistent with those found in the heptapeptide. Biasing the list toward compounds that had overall dimensions suitable to fit within the binding groove reduced the resulting library of potential groups further. From this approach, the structurally most interesting group to emerge was 2-aminomannose, a sugar residue. The peptide−sugar hybrid prepared from 2-aminomannose (**43**) was significantly more potent than the parent tetrapeptide **39**. Other amino sugar derivatives such as **44**, **45**, and **46** were no more potent than the parent tetrapeptide **39**, suggesting specific interactions could be responsible for the increased activity. *While sugars have been employed as scaffolds for peptide mimetics designs,[20] this appears to be the first instance of a sugar replacing amino acids in a peptide ligand.* Extending this finding, we also simplified the structure to diethanolamine and ethanolamine appendages attached to pentapeptide-sized ligands, in **48** and **49**, respectively. These hydroxyalkyl-pentapeptides were generally equivalent in potency to hexapeptides **35** and **41**, ending in Ser-$NH_2$, or to heptapeptides **1** and **40**, ending in a Ser-Leu-$NH_2$ sequence (Table 5), and were superior in binding to the pentapeptides **36** and **42**.

**Table 5.** Structures and Binding Data for Mannose, Serinol, and Ethanolamine Tetrapeptide Analogues

| | | mean relative potency | |
|---|---|---|---|
| no. | structure | DRB1-*0401 | DRB-*0101 |
| **40** | Ac-(Cha)RMMASL-$NH_2$ | 0.88 | 1.05 |
| **41** | Ac-(Cha)RMMAS-$NH_2$ | 0.85 | 1.38 |
| **42** | Ac-(Cha)RMMA-$NH_2$ | 0.15 | 0.59 |
| **43** | Ac-(Cha)RMM-(mannosamine) | 0.81 | 0.50 |
| **44** | Ac-(Cha)RMM-(galactosamine) | 0.16 | 0.12 |
| **45** | Ac-(Cha)RMM-(aminomannopyranoside) | 0.17 | 0.24 |
| **46** | Ac-(Cha)RMM-(aminoglucopyranoside) | 0.11 | 0.13 |
| **47** | Ac-(Cha)RMM-(normetanephrine) | 0.11 | 0.23 |
| **48** | Ac-(Cha)RMMA-$NHCH(CH_2OH)_2$ | 1.55 | 0.68 |
| **49** | Ac-(Cha)RMMA-$NHCH_2CH_2OH$ | 1.04 | 0.33 |

[a] Ratio of $IC_{50}$ values for Ac-(Cha)RAMASL-$NH_2$ and listed sequences. Values greater than 1 are more potent.

***N*-Methylation To Probe Backbone Recognition and Stabilize toward Enzymatic Cleavage.** An approach to dissect the relative contributions of backbone amides to conformational and H-bond donor properties of a peptide is to *N*-alkylate the secondary amide bonds. This modification has been shown to affect the conformation of peptides by supporting both left-handed and extended conformations of a peptide and to promote cis−trans isomerization. The tertiary amide formed by *N*-methylation is incapable of hydrogen bonding through the nitrogen and would project a hydrophobic group into a location previously occupied only by a hydrogen atom.[21] Because of this, the effect of *N*-alkylation on a biological property has to be interpreted with caution, since multiple effects (conformational, steric, and lack of a H-bond donor) could affect binding. X-ray data[4] suggests that *N*-methylation might be tolerated at some sites. To confirm which backbone amide bonds contribute or do not participate in binding to the class II MHC, a series of *N*-methyl analogues of Ac-(Cha)RAMASL-$NH_2$ was prepared and tested for effect on binding. The

**Table 6.** *N*-Methyl Scan of Ac-(Cha)RAMASL-$NH_2$

| | | mean relative potency[a] | |
|---|---|---|---|
| no. | structure | DRB1*0401 | DRB1*0101 |
| **32** | Ac-(Cha)RAMAS(MeL)-$NH_2$ | 0.77 | 0.85 |
| **50** | Ac-(Cha)RAMA(MeS)L-$NH_2$ | 0.97 | 0.50 |
| **51** | Ac-(Cha)RAM(MeA)SL-$NH_2$ | 0.60 | 1.22 |
| **52** | Ac-(Cha)RA(MeM)ASL-$NH_2$ | 0.005 | 0.046 |
| **53** | Ac-(Cha)R(MeA)MASL-$NH_2$ | 0.56 | 1.02 |
| **54** | Ac-(Cha)(MeR)AMASL-$NH_2$ | 0.001 | 0.001 |
| **55** | Ac-(MeCha)RAMASL-$NH_2$ | 0.67 | 0.25 |

[a] Ratio of $IC_{50}$ values for Ac-(Cha)RAMASL-$NH_2$ and listed sequence. Values greater than 1 are more potent.

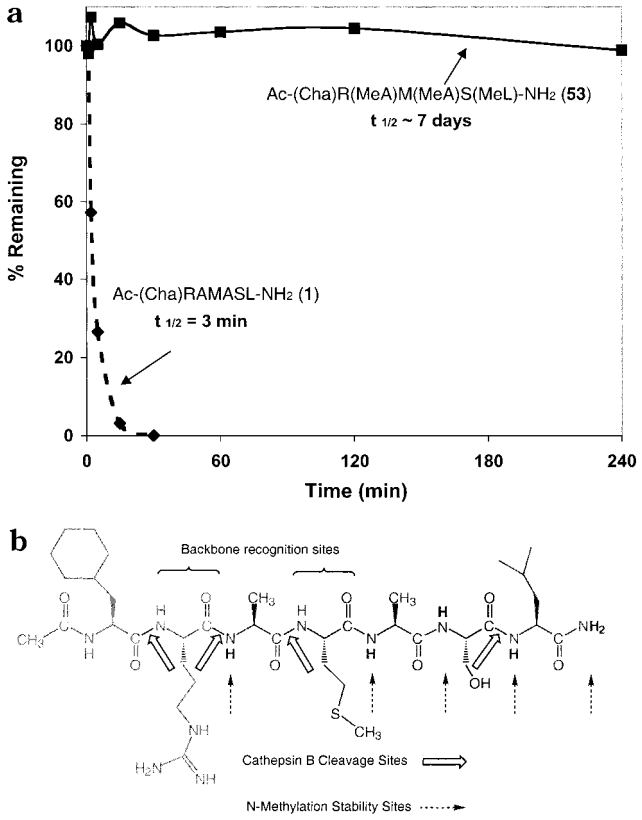


**Figure 6.** (a) Time course of cleavage of Ac-(Cha)RAMASL-$NH_2$ (**1**) and the trimethylated analogue (**57**) by cathepsin B. (b) Allowed *N*-methylation sites, backbone recognition residues, and cathepsin B cleavage sites for **1**.

results for the "*N*-methyl scan"[22] are shown in Table 6 and Figure 6b.

Methylation of the amide nitrogens at residues 1, 3, 5, 6, and 7 produces minimal effect on the binding to the DRB1*0401 and DRB1*0101 proteins. For methylation at positions 2 and 4 the effect was dramatically different. At both of these sites, the resulting compounds, **54** and **52**, were found to have 1000−200-fold decreased binding. These results support the X-ray crystallography data[4] indicating that the amide N−H functionalities are involved in critical hydrogen bonding to the class II MHC proteins and cannot be replaced without compromising ligand recognition. Peptide mimetics which are designed to replace any of the key backbone recognition sites must retain the appropriate hydrogen-bond donor and acceptor groups (from positions 2 and 4) or surrogates for them. The results from the *N*-methyl scan also demonstrate that none of the other backbone NH groups are required for binding, and this can be observed at p3 in two of our crystal structures, **73** and **60**, where the NHs are methylated. In both cases, the position of the methyl group is coincident with the calculated placement of the hydrogen of the nonmethylated residues of compounds **28** and **72** in their crystal structures.

**Table 7.** Cathepsin B Degradation of Selected *N*-Methylated Heptapeptides

| | | cathepsin B degradation | |
|---|---|---|---|
| no. | structure | % at 4 h[a] | half-time |
| **1** | Ac-(Cha)RAMASL-$NH_2$ | 0 | 3 min |
| **32** | Ac-(Cha)RAMAS(MeL)-$NH_2$ | 0 | 4.6 min |
| **51** | Ac-(Cha)RAM(MeA)SL-$NH_2$ | 0 | 7.3 min |
| **56** | Ac-(Cha)RAM(MeA)S(MeL)-$NH_2$ | 0 | 4.8 min |
| **57** | Ac-(Cha)R(MeA)M(MeA)S(MeL)-$NH_2$ | 99 | 7.4 days |

[a] Percentage of original compound remaining after 4 h incubation.

## Cathepsin B Degradation

The antigen processing and loading compartments of antigen presenting cells are occupied by a series of cysteine proteases, in particular cathepsins B, D, E,[23] L, and S.[24,25] For any compound to be an effective inhibitor of T-cell recognition, it must compete inside the endosomal compartments against peptide fragments produced from native antigen and, of necessity, must survive in the environment of APC endosomes. Among the cathepsins tested (B, D, L), we have found that Ac-(Cha)RAMASL-$NH_2$ is rapidly degraded by one of these enzymes, cathepsin B. It was determined that this enzyme, acting as both an endopeptidase and carboxydipeptidase, cleaves the peptide at several amide bonds. Figure 6b illustrates the cleavage sites identified between residues 2−3, 4−5, and 6−7. An assay was designed to determine the stability of various compounds toward cathepsin B and used to screen for potential cellular stability. Compounds were analyzed using HPLC, for the amount of material remaining intact during incubation, at several time points, and an assessment of degradation half-time was obtained (see Table 7).

We hypothesized that protection against cathepsin B cleavage in vitro might correlate with increased efficacy in cellular assays. To test the validity of this hypothesis, a triply methylated compound was prepared which incorporated *N*-methyl groups at each of the critical cleavage sites. Ac-(Cha)R(MeA)M(MeA)S(MeL)-$NH_2$, **57**, was found to possess somewhat reduced binding affinity for DRB1*0401 and DRB1*0101 with relative potencies of 0.30 and 0.48, respectively. However, when this compound was tested for cathepsin B stability, it was found to be completely stable in vitro over a 24-hour test period (see Figure 6a). The calculated half-time for degradation was measured in days, whereas the unprotected peptide had a half-life of 3 min under the conditions of the assay.

*N*-methylations, or other substitutions described below that prevent cathepsin B cleavage, opened the doorway to cellular activity in models of T-cell proliferation induced by protein antigens. Our interpretation was that the *N*-methylations permitted the compounds to survive in the endosomal compartment, where antigenic proteins are being degraded into peptide antigens, and that the stabilized *N*-methyl peptides were thus able to compete effectively with loading of the MHC molecule

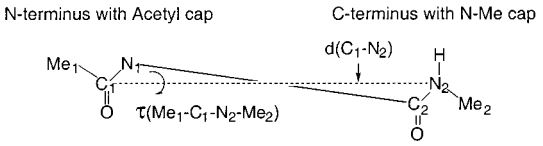


For HA (307-319) peptide in DRB1*0101 X-ray:

| position | d, A | τ, deg |
|---|---|---|
| 2-3 | 7.443 | -103.6 |
| 4-5 | 7.439 | -98.3 |

**Figure 7.** Conformational considerations for dipeptide mimetics in MHC class II binding site.

and to antagonize T-cell responses to antigenic peptides.[10] Our data does not rule out a role for other cathepsins but suggests that stabilization toward cathepsin B also protects against cleavage by other by other members of the class.

## Dipeptide Mimetics

A number of dipeptide mimetic structures have been described in the literature, and many have found utility in the context of peptide-based enzyme inhibitors or as templates for mimicry of specific peptide conformations. Conformational properties of many examples have recently been reviewed and cataloged.[26] In that analysis, the distances between the bond vectors in the peptide sequence to be replaced by the mimetic and the pseudotorsion angle between the incoming and exiting bond vectors were characterized for low-energy conformers. The approach can serve to identify potential mimetics whose backbone conformations are consistent with a reference peptide (Figure 7). In the present case, we need not only to maintain incoming and exiting bond vectors but also maintain backbone H-bonding at p2 and p4. As shown from the *N*-methylation scan, peptide mimetics which are designed to replace any of the key backbone recognition sites must retain the appropriate hydrogen-bond-donor and -acceptor groups (from positions 2 and 4) or surrogates for them. With this constraint, we chose to identify suitable dipeptide mimetics for replacement of residues at p2−3, p4−5, and p6−7. For p6−7 a similar approach of designing spacers with appropriate distance and side chain requirements was undertaken.[27]

Using such a strategy, the distances to be spanned and the corresponding pseudotorsion angles in the DRB1*0101 crystal structure at positions 2−3 and 4−5 were found to be similar and could potentially be matched by the same mimetic used in either site. There is a wide array of compounds classified as dipeptide mimetics that have the distance, torsion angle, and hydrogen-bonding potential to be used in replacements of the MHC peptide backbone. Figure 8 shows the series we incorporated into the sequence at either positions 2−3, 4−5, or both. We found that the 7,6 bicyclic pyridizine, 9-aminooctahydro-6,10-dioxo-6*H*- pyridazino-[1,2-*a*][1,2]diazepine-1-carboxylic acid (Odapdc) and a 5-amino-1,2,4,5,6,7-hexahydroazepino[3,2,1-*hi*]indol-4-one-2-carboxylic acid (Haic) were suitable replacements. As can be seen, both Haic and Odapdc can maintain backbone H-bonds at p2 or p4. Odapdc led to compounds active in binding assays for both sites, but not in combination (probably due to steric interactions of the two mimetics), whereas Haic was active only in the 4−5 position and did not work in combination with Odapdc in the 2−3 position. The binding affinities of these replacements were less than the corresponding natural dipeptide, but the improved stability of the 4−5 Haic analogues toward enzymatic degradation was translated into good activity in inhibition of T-cell proliferation in response to protein antigens, particularly when combined with *N*-methyls or other nonnatural residues. We have examples of each of the dipeptide mimetics in the 4−5 positions in our crystal structures (Figure 5); compound **72** has Odapdc and **73** has Haic. In each case, the backbone of the mimetic precisely follows the backbone of the peptides, as in our crystal structures with compounds **28** and **60**. Additionally, the pucker of

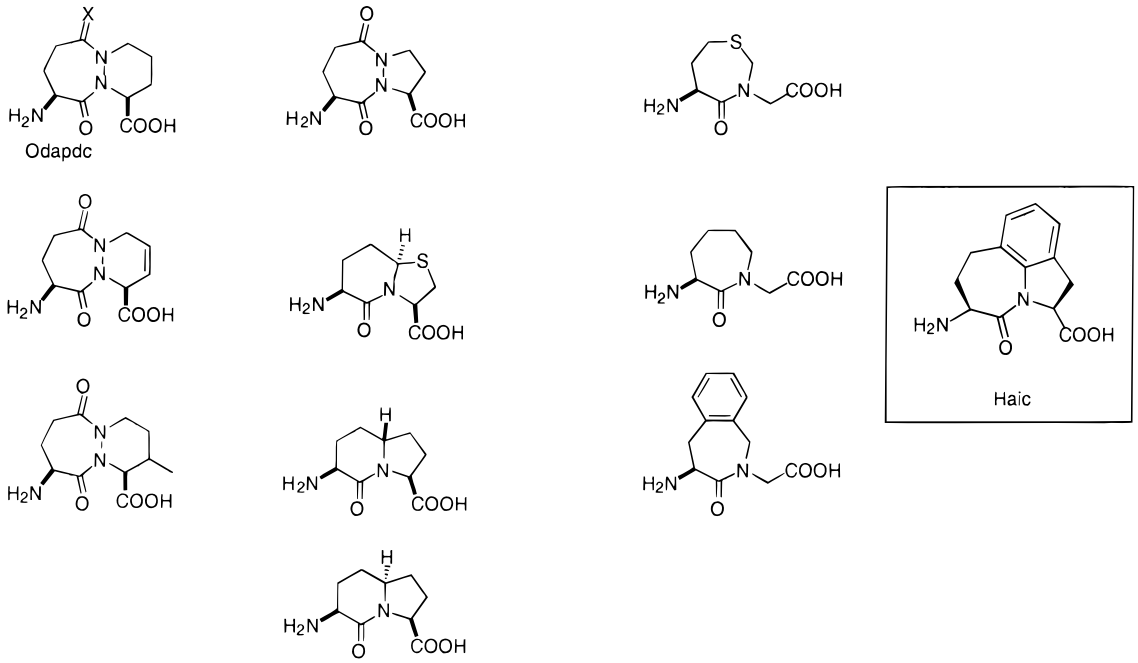


**Figure 8.** Dipeptide mimetic structures employed in backbone replacements of Ac-(Cha)RAMASL-$NH_2$.

**Table 8.** Combinations of Substitutions and Dipeptide Mimetics Used in the Preparation of Stabilized Ligands

| X-$A_1$-$A_2$-$A_3$-$A_4$-$A_5$-$A_6$-$A_7$-Y | | | | | | | | |
|---|---|---|---|---|---|---|---|---|
| X | $A_1$ | $A_2$ | $A_3$ | $A_4$ | $A_5$ | $A_6$ | $A_7$ | Y |
| $CH_3CO$ | Cha | Arg | MeAla | Met | MeAla | Ser | Leu | NH2 |
| $NH_2(CH_2)_4CO$ | 4-MeCha | His | MePhg | Nle | $\beta$-PhePro | | tLeu | NMe2 |
| $NH_2(CH_2)_3CO$ | Nba | $Orn(Me)_2$ | Tic | Chg | Pro | | MeLeu | |
| Ac-Lys | Coa | aIle | Thiq | | | | | |
| MorphCO | | Ile | Disc | | | | | |
| Val | | | | | | | | |
| Nle | | | | | | | | |
| Odapdc | | | Haic | | | | | |
| Odapdc | | | | | | | | |

**Table 9.** Summary of Results for *N*-Methylated, Dipeptide-Mimetic, and Combination Peptides

| | | mean rel pot.[a] | | % cathepsin | T-cell inhibition[c] | |
|---|---|---|---|---|---|---|
| no. | structure | *0401 | *0101 | B[b] at 4 h | *0401 | *0101 |
| **1** | Ac-(Cha)RAMASL-$NH_2$ | 1.00 | 1.00 | 0 | inact. | 0.12 |
| **58** | Ac-(Cha)R(MeA)(Haic)S(MeL)-$NH_2$ | 0.18 | 0.03 | 106 | 2.32 | <0.04 |
| **59** | Ac-(Cha)R(Tic)M(MeA)S(MeA)-$NH_2$ | 1.05 | 0.89 | 99 | 1.5 | 0.86 |
| **60** | Ac-(Cha)R(MePhg)MAS(tLeu)-$NH_2$ | 2.02 | 1.15 | 93 | 3.2 | 5.37 |
| **61** | Ac-(Cha)R(tLeu)M(MeA)S(tLeu)-$NH_2$ | 0.38 | 0.29 | 97 | 1.5 | 2.9 |
| **62** | Ac-(Cha)R(MeA)M($\beta$-PhPro)S(MeA)-$NH_2$ | 0.20 | 0.32 | 106 | 1.2 | 3.7 |
| **63** | Ac-(Cha)R(MePhg)(Haic)S(MeA)-$NH_2$ | 0.37 | 0.01 | 141 | 4.6 | <0.2 |
| **64** | Ac-(Cha)R(MePhg)(Haic)S(tLeu)-$NH_2$ | 0.23 | 0.06 | 126 | 3 | 2.3 |
| **65** | Ac-(Cha)R(Tic)(Haic)S(MeA)-$NH_2$ | 0.27 | 0.12 | 109 | 0.7 | 0.2 |
| **66** | Ac-(Cha)R(Tic)M($\beta$-PhPro)S(MeA)-$NH_2$ | 0.63 | 0.84 | 98 | 4.6 | 6.9 |
| **67** | Ac-(Cha)R(MePhg)M(MeA)S(tLeu)-$NH_2$ | 1.27 | 1.64 | 43 | 2.5 | 7.8 |
| **68** | Ac-(Cha)R(MePhg)(Haic)S(MeL)-$NH_2$ | 0.11 | 0.01 | 95 | 1 | 0.1 |
| **69** | Ac-(Cha)R(MeA)M($\beta$-PhPro)S(tLeu)-$NH_2$ | 0.54 | 0.94 | 106 | 4 | 3.9 |
| **70** | Ac-(Cha)R(Tic)M($\beta$-PhPro)S(MeL)-$NH_2$ | 0.22 | 0.49 | 116 | 2.7 | 2.5 |
| **71** | Ac-(Cha)R(Tic)M($\beta$-PhPro)S(tLeu)-$NH_2$ | 0.64 | 0.94 | 121 | 6.5 | 5.8 |

[a] Ratio of $IC_{50}$ values for Ac-(Cha)RAMASL-$NH_2$ and listed compound. [b] Percentage of compound remaining after incubation with cathepsin B for 4 h. [c] Ratio of $IC_{50}$ values for a(Cha)AAAKTAAAAa-$NH_2$ and listed compound.

the seven-membered rings in Haic and Odapdc aligns their methylene groups with the C$\beta$ and C$\gamma$ atom positions of the Met side chains in compounds **28** and **60**.

The relative potencies for compounds **72** and **73** are 10- and 100-fold less, respectively, for DRB1*0101 than for DRB1*0401. We attribute this difference in potency to interactions with the $\beta$ chain p71 groups. Thus, interaction with Lys-71 of DRB1*0401, which makes a hydrogen bond with the carbonyl oxygen of the dipeptide mimetics, is acceptable for both Odapdc and Haic and allows sufficient space for their fused ring systems. In addition, the aromatic ring of the Haic group is nicely positioned to form a $\pi$-cation interaction with Lys-71. However, in DRB1*0101, residue $\beta$71 is Arg, and although it makes similar contacts with the peptide carbonyl at position 5 as the Lys, it is too large to fit its larger side chain against the bulky ring systems of the mimetics. This steric conflict is greatest in the Haic analogue, where the aromatic ring and guanidine would have to occupy the same space.

## Inhibition of T-cell Proliferation by Mimetics

Combinations of the modified amino acids and dipeptide mimetics described above were explored to identify analogues with good affinity in binding, complete resistance to cathepsin B, and solubility properties suitable for the cellular assay conditions. The matrix of substitutions consistent with activity in inhibition of T-cell responses is shown in Table 8. A series of compounds was prepared in a combinatorial manner. From over 300 analogues, several displayed properties suitable for further testing for inhibition of T-cell proliferation (Table 9). T-cell inhibitory potency was measured relative to the $IC_{50}$ of a(Cha)AAAKTAAAAa-$NH_2$ (ca. 5 $\mu$M). In general, compounds that retained significant binding affinity for DRB1*0401 or -*0101 and were stable to cathepsin B under the assay conditions were able to inhibit T-cell responses to presented peptide antigen in DRB1*0401 and -*0101 clones, respectively.[10] Compounds that showed a selectivity for inhibition of one allele over the other in the binding assay, such as **63** or **68**, tended to also show selective inhibition of T-cell proliferation. Compounds that showed high binding affinity for *0401 and *0101 and were not stable to cathepsin B, yielded poor activity for inhibition of T-cell responses (data not shown).

The most potent analogues were further tested for inhibition of T-cell response of HEL-specific polyclonal T-cells and OVA-specific T-cell hybridomas derived from HLA-DR4-IE chimeric, transgenic mice.[10] One of the more potent compounds in this assay, Ac-(Cha)R(Tic)M-($\beta$-PhPro)S(MeL)-$NMe_2$, **70**, was found to be 2030 and 204 times more potent than the parent heptapeptide, **1**, in inhibiting the T-cell proliferation. This clearly indicates that a small peptidomimetic, properly stabilized to metabolic degradation, can block a T-cell response to a processed protein antigen.

## Summary and Conclusions

In this work, peptide structure−activity studies and structure-based drug design have been employed to elucidate molecular features of ligand binding to MHC class II HLA-DR molecules. At the same time, consideration of factors responsible for antigen processing led to the selection of compounds with stability toward

cathepsin B. Such analogues were able to compete effectively against protein antigens in cellular assays, resulting in inhibition of T-cell proliferation. X-ray structures of four complexes of peptide-MHC DR4-SEB having diverse mimetic replacements revealed additional interactions. The structural data also led to the design of an interesting peptide−sugar hybrid. These studies illustrate the complementary roles played by phage display library methods, peptide analogue SAR, peptide mimetics substitutions, and structure-based drug design in the discovery of inhibitors of antigen presentation by HLA-DR molecules. Future work will determine the in vivo responses and effects of such inhibitors in autoimmune disease models and could lead to useful therapeutic agents.

## Experimental Section

**Abbreviations.** Single letter or three letter codes are used for the standard amino acids. For single letter codes, uppercase signifies the natural L configuration, whereas lowercase signifies the D configuration. Abbreviations for amino acids and dipeptide mimetics used: Ac, acetyl; Cha, cyclohexylalanine; $pCH_3$-Cha, *p*-methylcyclohexylalanine; Nba, norbornylalanine; Coa, cyclooctylalanine; aIle, allo-isoleucine; $Orn(Me)_2$, $N^{\delta}$,$N^{\delta}$-dimethylornithine; $Lys(Me)_2$, $N^{\epsilon}$,$N^{\epsilon}$-dimethyllysine; Phg, phenylglycine; MePhg, *N*-methylphenylglycine; Chg, cyclohexylglycine; Tic, tetrahydroisoquinoline-(S)-3-carboxylic acid; Disc, dihydroisoindole-(*S*)-2-carboxylic acid; Thiq, tetrahydroisoquinoline-(*S*)-1-carboxylic acid; β-PhPro, 3-phenylproline; Haic, 5-amino-4-oxo-1,2,4,5,6,7-hexahydroazepino[3,2,1-*hi*]indole-2-carboxylic acid; Odapdc, 9-amino-6,10-dioxo-octahydropyridazino[1,2-*a*][1,2]diazepine-1-carboxylic acid; tLeu, *tert*-leucine; Mdp, 3,4-methylenedioxyphenylalanine; Bcoa, (2*S*)-amino-3-((2*S*)-bicyclo[2.2.2]oct-2-yl)propionic acid; Pip, pipecolic acid; aminoglucopyranoside, methyl 3-amino-3-deoxy-β-D-glucopyranoside; aminomannopyranoside, methyl 3-amino-3-deoxy-α-D-mannopyranoside; normetanephrine, α-[aminomethyl]-4-hydroxy-3-methoxybenzenemethanol. Other abbreviations used: MHC, major histocompatibility complex; SEB, staphylococcal enterotoxin B from *Staphylococcus aureus*.

**General.** HPLC chromatography was performed on an LDC apparatus equipped with two Constametric pumps, a Gradient Master solvent programmer and mixer, and a Spectromonitor III variable wavelength UV detector. Preparative HPLC separations were run on a Whatman Magnum 20 partisil 10 ODS-3 column (2 × 50 cm) equipped with a Waters Guard-Pak $C_{18}$ precolumn. For amino acid composition analyses, peptides were hydrolyzed in 6 N HCl, containing 4% thioglycolic acid, at 115 °C for 22 h in sealed, evacuated hydrolysis tubes. Analyses were performed on a Waters HPLC-based amino acid analysis system using an AA511 column (Interaction Chromatography, San Jose, CA) and postcolumn ninhydrin detection. Fast-atom bombardment mass spectra (FAB-MS) were obtained on a VG 70E-HF or VG AutoSpec mass spectrometer. Electrospray mass spectra (ES-MS) were obtained on a VG Platform mass spectrometer.

**Reagents.** Unless otherwise stated, all reagents and solvents were obtained commercially as reagent grade and used without further purification. Water for HPLC was prepared from doubly deionized, filtered water and purified on a Hydro Services purification unit. Fmoc-protected amino acids were purchased from Bachem (Torrance, CA), Advanced ChemTech (Louisville, KY), or SNPE. Those not commercially available (Odapdc,[28] Disc,[29] β-phePro[30]) were prepared according to literature procedures. BHA resin (100−200 mesh) was obtained from Bachem. Rink linker was purchased from Nova-Biochem (CA) and coupled to BHA resin using DIC/HOBT.

**Peptide and Peptidomimetic Synthesis.** Peptides and analogues incorporating peptidomimetic were generally prepared using solid-phase synthesis procedures as described by Barany and Merrifield.[31] All amino acids were protected as the $N^{\alpha}$-Fmoc derivatives. For the synthesis of C-terminal amides Fmoc−Rink linker−BHA resin[32] was used. For the synthesis of C-teminal acids Wang resin[33] was used. In general, all amino acids were coupled using either the HBTU/HOBT or DIC/HOBT protocols. Couplings to *N*-alkyl or imino acids were performed with either BOP-Cl or PyBrOP in NMP. The Fmoc groups were removed using 20−40% piperidine in DMF.

Peptides were deblocked and cleaved from the resin by treating with a mixture of TFA, ethanedithiol, dimethyl sulfide, and anisole at room temperature for 2 h. The resin was filtered and washed, and the combined filtrates were precipitated in 25−100 mL of $Et_2O$. The precipitated solid was centrifuged down, washed with two 20 mL volumes of $Et_2O$, and dried under vacuum. When racemic amino acids were employed in coupling steps, individual diastereoisomers were isolated by HPLC and tested independently. The inactive member of a diasteriomeric pair was assumed to have an unnatural configuration based on previous D-scans that established the requirement for all L-amino acid peptides (data not shown).

Purification was carried out by preparative HPLC. The peptides were applied to the column in a minimum volume of either 10−20% AcOH or 0.1% TFA. Gradient elutions were performed using linear gradients of buffer A (0.1% TFA/$H_2O$) and buffer B (0.1% TFA/$CH_3CN$) at a flow rate of 8.0 mL/min with UV detection at 220 nm. Fractions were collected at 1.5−2.5 min intervals, inspected by analytical HPLC, pooled, and lyophilized.

The final products were characterized by analytical HPLC, FAB-MS, and/or ES-MS and amino acid analysis. HPLC purity, as determined from all UV active peaks, was typically greater than 97%. The expected parent M + H ions and amino acid composition values were obtained within acceptable limits.

**Cathepsin B Degradation.** Compounds were weighed, approximately 0.3 mg each, into centifugal-filter vials. The samples were dissolved in pH 6.0 phosphate buffer (88 mM $KH_2PO_4$, 12 mM $Na_2HPO_4$, and 1.33 mM EDTA in deionized $H_2O$ brought to pH 6.0 with 1.0 N NaOH and containing 2.0 mM cysteine and 0.1% by volume 4-isopropylbenzyl alcohol as an HPLC internal standard) to give concentrations of 1.0 mg/mL. Cathepsin B was activated by taking a 1.0 U frozen aliquot [10 units of cathepsin B, obtained as a lyophilized powder (Sigma cat #C6286), were dissolved in 500 μL of 0.1 mM $HgCl_2$, and 1.0 U aliquots (50 μL) were transferred to screw-cap vials and immediately frozen.], diluting it with 50 μL of activation buffer (containing 1.0 mM EDTA) and warming it to 37 °C for 5 min. The enzyme was placed on ice until used. The prewarmed (32 °C) sample solutions were incubated with 0.3 U of enzyme per micromole of compound. Then, 100 μL aliquots of solution were withdrawn at time points 0, 1, 2, 5, 15, 30, 60, 120, 240, and 1440 min after introduction of the enzyme. The aliquots were pipetted into autosampler vials and immediately quenched with 10 μL of 50% TFA solution and chilled on ice.

The aliquots from each time point were analyzed by analytical HPLC using a YMC-AQ $C_{18}$ 3 μm column (0.4 × 10 cm) with a linear gradient of buffer A (0.05% TFA/$H_2O$) and buffer B (0.04% TFA/$CH_3CN$) from 10 to 65% B in 10.5 min at 1.0 mL/min flow rate. The eluent was monitored by UV at 210 nm and 0.2 AUFS and integration of the chromatogram was performed using a Hewlett-Packard Model 3310 recording integrator.

The relative concentration of each compound could be estimated from the integration of the area under each sample peak. Sampling errors were minimized by factoring each area by the area of the corresponding internal standard. The half-times for degradation were estimated by plotting % remaining ($A/A_o \times 100$) vs time. Alternatively, the half-times could be calculated from a plot of $\ln(A_o - A)$ vs time, where $t^{1/2} = 0.693/k$.

**Peptide Binding Assay.** A scintillation proximity assay (SPA) format was developed for high-throughput screening of DR-binding compounds as described previously.[10] Briefly, an $^{125}$I-labeled peptide, YAAFRAAASAKAAA-$NH_2$, was used as

**Table 10.** X-ray Diffraction Data Statistics

| no. | structure | resolution (Å) | no. refls/completeness | $R_{merge}$ |
|---|---|---|---|---|
| **28** | Ac-(Cha)RAM(CAcm)SL-$NH_2$ | 20−2.0 | 50 025/94.5% | 0.078 |
| **72** | Ac-(Cha)RA(Odapdc)SL-$NH_2$ | 20−2.0 | 51 927/96.2% | 0.067 |
| **73** | Ac-(Cha)R(MeA)(Haic)-NHCH($CH_2OH$)$_2$ | 20−2.45 | 38 325/99.4% | 0.095 |
| **60** | Ac-(Cha)R(MePhg)MAS(tLeu)-$NH_2$ | 20−2.45 | 31 200/97.7% | 0.055 |

**Table 11.**

(a) Summary of Data from Molecular Replacement Using AMoRe

| | |
|---|---|
| space group | $P2_12_12_1$ |
| search probe | DR1(all atoms)/SEB(main chain atoms) |
| resolution | 15−3 Å |
| *R* factor | 44.9 (second peak − 49.5) |
| correlation coefficient | 26.3 (second peak − 12.0) |

(b) Unit Cell Parameters and Refinement Results

| | | unit cell parameters (Å) | | | | | |
|---|---|---|---|---|---|---|---|
| no. | resolution (Å) | *a* | *b* | *c* | *R* value | $R_{free}$ | no. atoms/no. refls |
| **28** | 2.0 | 82.38 | 93.94 | 99.68 | 0.236 | 0.260 | 5077/48815 |
| **72** | 2.0 | 78.34 | 100.17 | 100.21 | 0.234 | 0.265 | 5045/50725 |
| **73** | 2.45 | 90.84 | 104.25 | 107.82 | 0.242 | 0.272 | 5026/35655 |
| **60** | 2.45 | 80.83 | 102.34 | 102.7 | 0.198 | 0.226 | 4926/30746 |

a radioligand to bind to monoclonal antibody (LB3.1) purified DR protein (DRB1*0101, DRB1*0401, or DRB1*0404). Test compounds were used as competitors against the radioligand. DR molecules were captured with biotinylated Mab LB3.1 on avidin-coated SPA beads (Amersham Corp., Arlington Heights, IL), and the DR-bound radioactivity was measured directly by scintillation counting. Ac-(Cha)RAMASL-$NH_2$ was run in each assay as a standard competitor. Potency is reported relative to the standard within each assay run.

**Assay for Competition for Antigen Presentation.** The competition assays were performed as described previously.[10,34]

**X-ray Crystallography.** DRA/DRB1*0401 was isolated from baculovirus-infected Hi-5 insect cells according to the procedure described by Stern et al.[4] for DRA/DRB1*0101. Lyophilized SEB (Sigma, 31% protein) was dissolved in 10 mM Tris pH 7.4, mixed with soluble DR4 peptide complex at a 1:3 ratio of DR4:SEB, and incubated overnight at 4 °C. The ternary complex was then concentrated to 15 mg/mL. Crystals were grown at 20 °C from hanging drops composed of a 1:1 mixture of protein with a reservoir solution consisting of 5% PEG 4000, 10 mM sodium acetate, at pH 5, and 2.4% ethylene glycol. Crystals composed of DR4/SEB complex with **28** and **72** were transferred into a cryosolution for data collection by gradual transfer into 20% PEG 4000, 12−16% glycerol, 2.5% ethylene glycol, 10 mM sodium acetate, pH 5, and frozen in a −160 °C nitrogen gas stream. X-ray diffraction data were collected using Fuji image plates at the HHMI X-4A beamline of the National Synchrotron Light Source at Brookhaven National Laboratory at a wavelength of 0.9686 Å. Crystals containing DR4/SEB in complex with **73** and **60** were mounted in glass capillaries, and X-ray diffraction data were collected at room temperature using Cu Kα radiation with a MAR image plate on a Rigaku rotating anode generator. Data are summarized in Table 10. The X-ray diffraction data for all crystals were processed and scaled using Denzo and Scalepack.[35] The atomic coordinates of DR4/SEB in complex with compound **28** (code 1D5M), **72** (code 1D5Z), **73** (code 1D5X), and **60** (code 1D6E) have been deposited at the Protein Data Bank.

The structure of DR4/SEB/**28** was solved by molecular replacement using AmoRe[36] and data in the resolution range of 15−3 Å. The search probe was derived from the complex of DR1/SEB[37] and included all atoms of DR1 and only the main chain atoms of SEB. The molecular replacement results are given in Table 11a. All atoms of the DR1/SEB model (Jardetsky et al.[4b]) were oriented according to the molecular replacement solution. The SEB coordinates from this complex are missing several segments; therefore, a more complete SEB coordinate set corresponding to a 2.5 Å resolution structure was obtained from Swaminathan[38] and used to replace the SEB coordinates of the DR1/SEB complex. Side chains unique to DR1 were replaced with DR4 side chains. Structure refinement was performed using X-plor[39] followed by CNS[40] with final *R*-values given in Table 11b. In the 2 Å DR4/peptide structure, electron density clearly indicated the presence of one unit of *N*-acetylglucosamine attached to Asn118. Sparse patches of electron density were observed in the vicinity of Asn200, the site of attachment of another carbohydrate moiety, but this was not modeled. The electron density for SEB was quite clear except for one loop from residue 99 to 108, which is disordered.

**Acknowledgment.** We thank Vance Bell and Teresa Burchfield for mass spectral analyses and Yu-Ching Pan and Doreen Ciolek for amino acid analyses.

**Supporting Information Available:** Table of MS data and amino acid analyses for compounds described and table of $IC_{50}$ values and relative potencies in HLA-DR binding assays for all compounds including those not specifically discussed but alluded to. This material is available free of charge via the Internet at http://pubs.acs.org.

## References

(1) Todd, J. A.; Acha-Orbea, H.; Bell, J. I.; Chao, N.; Fronek, Z.; Jacob, C. O.; McDermott, M.; Sinha, A. A.; Timmerman, L.; Steinman, L.; McDevitt, H. O. A molecular basis for MHC class II-associated autoimmunity. *Science* **1998**, *240*, 1003−1009.

(2) Tiwari, J.; Terasaki, P. *HLA and disease association*; Springer-Verlag: New York, 1985.

(3) Adorini, L.; Muller, S.; Cardinaux, F.; Lehmann, P. V.; Falcioni, F.; Nagy, Z. A. In vivo competition between self-peptides and foreign antigens in T-cell activation. *Nature* **1988**, *334*, 623−625.

(4) Stern, L. J., Brown, J. H.; Jardetzky, T. S.; Gorga, J. C.; Urban, R. G.; Strominger, J. L.; Wiley, D. C. Crystal structure of the human class II MHC protein HLA-DR1 complexed with an influenza virus peptide. *Nature* **1994**, *368*, 215−21. See also Jardetzky, T. S.; Brown, J. H.; Stern, L. J.; Urban, R. G.; Chi, Y.-I.; Stauffacher, C.; Strominger, J. L.; Wiley, D. C. Three-dimensional structure of a human class II histocompatibility molecule complexed with superantigen. *Nature* **1994**, *368*, 711−718. Ghosh, P.; Amaya, M.; Mellins, E.; Wiley, D. C. The structure of an intermediate in class II MHC maturation: CLIP bound to HLA-DR3. *Nature* **1995**, *378*, 457−462. Brown, J. H.; Jardetzky, T. S.; Gorga, J. C.; Stern, L. J.; Urban, R. G.; Strominger, J. L.; Wiley, D. C. Three-dimensional structure of the human class II histocompatibility antigen HLA-DR1. *Nature* **1993**, *364*, 33−39. Dessen, A.; Lawrence, C. M.; Cupo, S.; Zaller, D. M.; Wiley, D. C. X-ray crystal structure of HLA-DR4

(DRA0101, DRB10401) complexed with a peptide from human collagen II. *Immunity* **1997**, *7*, 473−481.

(5) (a) Garboczi, D. N.; Ghosh, P.; Utz, F.; Qing, R.; Biddison, W. E.; Wiley, D. C. Structure of the complex between human T-cell receptor, viral peptide and HLA-A2. *Nature* (London) **1996**, *384*, 134−141. (b) Garcia, K. C.; Degano, M.; Stanfield, R. L.; Brunmark, A.; Jackson, M. R.; Peterson, P. A.; Teyton, L.; Wilson, I. A. An $\alpha\beta$ T cell receptor structure at 2.5 Å and its orientation in the TCR-MHC complex. *Science* **1996**, *274*, 209−219. (c) Reinherz, E. L.; Tan, K.; Tang, L.; Kern, P.; Liu, J.; Xiong, Y.; Hussey, R. E.; Smolyar, A.; Hare, B.; Zhang, R.; Joachimiak, A.; Chang, H.; Wagner, G.; Wang, J. The crystal structure of a T-cell receptor in complex with peptide and MHC class II. *Science* **1999**, *286*, 1913−1921.

(6) (a) Hammer, J.; Takacs, B.; Sinigaglia, F. Identification of a motif for HLA-DR1 binding peptides using M13 display libraries. *J. Exp. Med.* **1993**, *176*, 1007−1013. (b) Hammer, J.; Valsasnini, P.; Tolba, K.; Bolin, D.; Higelin, J.; Takacs, B.; Sinigaglia, F. Promicsuous and allele-specific anchors in HLA-DR-binding peptides. *Cell* **1994**, *74*, 197−203. (c) Hammer, J.; Bono, E.; Gallazzi, F.; Belunis, C.; Nagy, Z. A.; Sinigaglia, F. Precise prediction of major histocompatibility complex class II-peptide interaction based on peptide side chain scanning. *J. Exp. Med.* **1995**, *180*, 2353−2358. (d) Hammer, J.; Gallazzi, F.; Bono, E.; Karr, R. W.; Guenot, J.; Valsasini, P.; Nagy, Z. A.; Sinigaglia, F. Peptide binding specificity of HLA-DR4 molecules: Correlation with rheumatoid arthritis association. *J. Exp. Med.* **1995**, *181*, 1847−1855.

(7) Lamont, A. G.; Powell, M. F.; Colon, S. M.; Miles, C.; Grey, H. M.; Sette, A. The use of peptide analogues with improved stability and MHC binding capacity to inhibit antigen presentation in vitro and in vivo. *J. Immunol.* **1990**, *144* (7), 2493−2498; See also ref 13.

(8) Ishioka, G. Y.; Adorini, L.; Guery, J. C.; Gaeta, F. C. A.; LaFond, R.; Alexander, J.; Powell, M. F.; Sette, A.; Grey, H. M. Failure to demonstrate long-lived MHC saturation both in vitro and in vivo. Implications for therapeutic potential of MHC-blocking peptides. *J. Immunol.* **1994**, *152* (9), 4310−4319.

(9) Siklodi, B.; Vogt, A. B.; Kropshofer, H,; Falcioni, F.; Molina, M.; Bolin, D. R.; Campbell, R.; Hammerling, G. J.; Nagy, Z. A. Binding affinity independent contribution of peptide length to the stability of peptide-HLA-DR complexes in live antigen presenting cells. *Hum. Immunol.* **1998**, *59* (8), 463−471.

(10) (a) Jones, A. B.; Acton, J. J.; Adams, A. D.; Yuen, W.; Nichols, E. A.; Schwartz, C. D.; Wicker, L. S.; Hermes, J. D. Tetrapeptide derived inhibitors of complexation of a class II MHC: fully unnatural ligands. *Bioorg. Med. Chem. Lett.* **1999**, *9*, 2115−2118. (b) Jones, A. B.; Acton, J. J.; Rivetna, M. N.; Cummings, R. T.; Cubbon, R. M.; Nichols, E. A.; Schwartz, C. D.; Wicker, L. S.; Hermes, J. D. Tetrapeptide derived inhibitors of complexation of a class II MHC: The peptide backbone is not inviolate. *Bioorg. Med. Chem. Lett.* **1999**, *9*, 2109−2114.

(11) Falcioni, F.; Ito, K.; Vidovic, D.; Belunis, C.; Campbell, R.; Berthel, S. J.; Bolin, D. R.; Gillespie, P. B.; Nuby, N.; Olson, G. L.; Sarabu, R.; Guenot, J.; Madison, V.; Hammer, J.; Sinigaglia, F.; Steinmetz, M.; Nagy, Z. A. Peptidomimetic compounds that inhibit antigen presentation by autoimmune disease-associated class II major histocompatibility molecules. *Nature Biotechnol.* **1999**, *17*, 562−567.

(12) (a) Hammer, J.; Valsasnini, P.; Tolba, K.; Bolin, D.; Higelin, J.; Takacs, B.; Sinigaglia, F. Promiscuous and allele-specific anchors in HLA-DR-binding peptides. *Cell* **1993**, *74*, 197−203. (b) Hammer, J.; Takacs, B.; Sinigaglia, F. Identification of a motif for HLA-DR1 binding peptides using M13 display libraries. *J. Exp. Med.* **1992**, *176*, 1007−1013.

(13) Hammer, J.; Belunis, C.; Bolin, D.; Papadopoulos, J.; Walsky, R.; Higelin, J.; Danho, W.; Sinigaglia, F.; Nagy, Z. A. High-affinity binding of short peptides to major histocompatibility complex class II molecules by anchor combinations. *Proc. Natl. Acad. Sci. U.S.A.* **1994**, *91*, 4456−4460.

(14) Smith, A. B., III; Benowitz, A. B.; Guzman, M. C.; Sprengeler, P. A.; Hirschmann, R.; Schweiger, E. J.; Bolin, D. R.; Nagy, Z.; Campbell, R. M.; Cox, D. C.; Olson, G. L. Design, synthesis and evaluation of a pyrrolinone-peptide hybrid ligand for the class II MHC protein HLA-DR1. *J. Am. Chem. Soc.* **1998**, *120*, 12704−12705.

(15) Smith, A. B., III; Benowitz, A. B.; Guzman, M. C.; Sprengeler, P. A.; Hirschmann, R.; Schweiger, E. J.; Bolin, D. R.; Nagy, Z.; Campbell, R. M.; Cox, D. C.; Olson, G. L. Design, synthesis and evaluation of a pyrrolinone-peptide hybrid ligand for the class II MHC protein HLA-DR1. *J. Am. Chem. Soc.* **1998**, *120*, 12704−12705.

(16) (a) Cunningham, B. R.; Rivetna, M.; Tolman, R. L.; Flattery, S. J.; Nichols, E. A.; Schwartz, C. D.; Wicker, L. S.; Hermes, J. D.; Jones, A. B. SAR for MHC class II binding tetrapeptides: Correlation with potential binding site. *Bioorg. Med. Chem. Lett.* **1997**, *7* (1), 19−24. (b) Acton, J. J., III; Adams, A. D.; Hermes, J. D.; Jones, A. B.; Parons, W. H.; Sinclair, P. J. Preparation of peptide lactams as inhibitors of peptide binding to MHC class II proteins. PCT Int. Appl., WO 9716425 A1 970509.

(17) Hanson, G. J.; Vuletich, J. L.; Bedell, L. J.; Bono, C. P.; Howard, S. C.; Welply, J. K.; Woulfe, S. L.; Zacheis, M. L. Design of MHC class II ligands using conformationally restricted imino acids at p3 and p5. *Bioorg. Med. Chem. Lett.* **1996**, *6*, 1931−36.

(18) Jones, A. B.; Acton, J. J., III; Rivetna, M. N.; Cummings, R. T.; Cubbon, R. M.; Nichols, E. A.; Schwartz, C. D.; Wicker, L. S.; Hermes, J. D. Tetrapeptide derived inhibitors of complexation of a class II MHC: The peptide backbone is not inviolate. *Bioorg. Med. Chem. Lett.* **1999**, *9*, 2109−14.

(19) Jones, A. B.; Acton, J. J., III; Adams, A. D.; Yuen, W.; Nichols, E. A.; Schwartz, C. D.; Wicker, L. S.; Hermes, J. D. Tetrapeptide derived inhibitors of complexation of a class II MHC: Fully unnatural ligands. *Bioorg. Med. Chem. Lett.* **1999**, *9*, 2115−18.

(20) (a) Hirschmann, R.; Nicolaou, K. C.; Pietranico, S.; Salvino, J.; Leahy, E. M.; Sprengeler, P. A.; Furst, G.; Strader, C. D.; Smith, A. B., III; et al. Nonpeptidal peptidomimetics with $\beta$-D-glucose scaffolding. A partial somatostatin agonist bearing a close structural relationship to a potent, selective substance P antagonist. *J. Am. Chem. Soc.* **1992**, *114*, 9217−18. (b) Hirschmann, R.; Nicolaou, K. C.; Pietranico, S.; Leahy, E. M.; Salvino, J.; Arison B.; Cichy, M. A.; Spoors, P. G.; Shakespeare, W. C.; et al. De novo design and synthesis of somatostatin non-peptide peptidomimetics utilizing $\beta$-D-glucose as a novel scaffolding. *J. Am. Chem. Soc.* **1993**, *115*, 12550−68.

(21) Manavalan, P.; Momany, F. A. Conformational energy studies on *N*-methylated analogues of thyrotropin releasing hormone, enkephalin, and luteinizing hormone-releasing hormone. *Biopolymers* **1980**, *19*, 1943−73.

(22) Miller, S. C.; Scanlon, T. S. Site-selective *N*-methylation of peptides on solid support. *J. Am. Chem. Soc.* **1997**, *119*, 2301−3.

(23) Bennett, K.; Levine, T.; Ellis, J. S.; Peanasky, R. J.; Samloff, I. M.; Kay, J.; Chain, B. M. Antigen processing for presentation by class II major histocompatibility complex requires cleavage by cathepsin E. *Eur. J. Immunol.* **1992**, *22* (6), 1519−24.

(24) Matsunaga, Y.; Saibara, T.; Kido, H.; Katunuma, N. Participation of cathepsin B in processing of antigen presentation to MHC class II. *FEBS Lett.* **1993**, *324* (3), 325−30.

(25) Bushell, G.; Nelson, C.; Chiu, H.; Grimley, C.; Henzel, W.; Burnier, J.; Fong, S.; Evidence supporting a role for cathepsin B in the generation of T cell antigenic epitopes of human growth hormone. *Mol. Immunol.* **1993**, *30* (6), 587−91.

(26) (a) Gillespie, P. Cicariello, J.; Olson, G. L. Conformational analysis of dipeptide mimetics, *Biopolm./Pept. Sci.* **1997**, *43*, 191−217. (b) Souers, A. J.; Virgilio, A. A.; Rosenquist, S. A.; Fenuik, W.; Ellman, J. A. Identification of a Potent Heterocyclic Ligand To Somatostatin Receptor Subtype 5 by the Synthesis and Screening of $\beta$-Turn Mimetic Libraries. *J. Am. Chem. Soc.* **1999**, *121* (9), 1817−1825.

(27) Sarabu, R.; et al., manuscript in preparation.

(28) Attwood, M. R.; Hassall, C. H.; Krohn, A.; Lawton, G.; Redshaw, S. The design and synthesis of the angiotensin-converting enzyme inhibitor cilazapril and related bicyclic compounds. *J. Chem. Soc., Perkin Trans. 1* **1986**, 1011−19.

(29) New, J. S.; Yevich, J. P. Synthesis of the 5*H*-pyrrolo[2,1-*a*]-isoindole ring with 1,3-dipolar cycloaddition reactions. *J. Heterocycl. Chem.* **1984**, *21* (5), 1355−60.

(30) (a) Herdeis, C.; Hubmann, H. P.; Lotter, H. Synthesis of homochiral 3-substituted glutamic acids and prolines from pyroglutamic acid. *Tetrahedron: Asymmetry* **1994**, *5* (3), 351-4. (b) Chung, J. Y. L.; Wasicak, J. T.; Arnold, W. A.; May, C. S.; Nadzan, A. M.; Holladay, M. W. Conformationally constrained amino acids. Synthesis and optical resolution of 3-substituted proline derivatives. *J. Org. Chem.* **1990**, *55* (1), 270−5.

(31) Barany, G.; Merrifield, R. B. Solid-phase peptide synthesis. In *The Peptides*; Gross, E., Meienhofer, J., Eds.; Academic Press: New York, 1980; Vol. 2, pp 1−284.

(32) Rink, H. Solid-phase synthesis of protected peptide fragments using a trialkoxy-diphenyl-methyl ester resin. *Tetrahedron Lett.* **1987**, *28*, 3787.

(33) Wang, S. S. p-Alkoxybenzyl resin and p-alkoxybenzylcarbonyl-hydrazide resin for solid-phase synthesis of protected peptide fragments. *J. Am. Chem. Soc.* **1973**, *95*, 1328−33.

(34) Falcioni, F.; Shah, H.; Vidovic, D.; Morimoto, C.; Belunis, C.; Bolin, D. R.; Nagy, Z. A. Influence of CD26 and integrins on the antigen sensitivity of human memory T cells. *Hum. Immunol.* **1996**, *50*, 79−90.

(35) Otwinowski, A.; Minor, W. Processing of X-ray diffraction data collected in oscillation mode, In *Methods in Enzymology*, *276A*; Carter, C. W., Jr., Sweet, R. M., Eds.; Academic Press: New York, 1997; pp 307−326.

(36) Navaza, J. AmoRe: An automated package for molecular replacement. *Acta Crystallogr. D* **1994**, *50*, 157−163.

(37) Jardetzky, T. S.; Brown, J. H.; Stern, L. J.; Urban, R. G.; Chi, Y.-I.; Stauffacher, C.; Strominger, J. L.; Wiley, D. C. Three-dimensional structure of a human class II major histocompatibility molecule complexed with superantigen. *Nature* **1994**, *369*, 711−718.
(38) Swaminathan, S.; Furey, W.; Pletcher, J.; Sax, M. Residues defining V beta specificity in staphylococcal enterotoxins. *Nat. Struct. Biol.* **1995**, *2*, 680−686.
(39) Brunger, A. T. *X-PLOR version 3.1: A system for X-ray crystallography and NMR*; Yale University Press: New Haven, CT, 1992.
(40) Brunger, A. T.; Adams, P. D.; Clore, G. M.; Delano, W. L.; Gros, P.; Grosse-Kunstleve, R. W.; Jiang, J.-S.; Kuszewski, J.; Nilges, N.; Pannu, N. S.; Read, R. J.; Rice, L. M.; Simonson, T.; Warren, G. L. Crystallography and NMR system (CNS): A new software system for macromolecular structure determination. *Acta Crystallogr.* **1998**, 905−921.

JM000034H